JOURNAL OF PHYSICAL ORGANIC CHEMISTRY
J. Phys. Org. Chem. 2007; **20:** 917–928
Published online 17 September 2007 in Wiley InterScience
(www.interscience.wiley.com) DOI: 10.1002/poc.1264

Photochromic crown-containing molecular switches of chemosensor activity

Vladimir A. Bren,[1] Alexander D. Dubonosov,[2]* Vladimir I. Minkin,[1] Alexey V. Tsukanov,[1] Tatyana N. Gribanova,[1] Evgenii N. Shepelenko,[2] Yurii V. Revinsky[1] and Vladimir P. Rybalkin[2]

[1]Institute of Physical and Organic Chemistry, Southern Federal University, Rostov on Don 344090, Russia
[2]Southern Scientific Center of Russian Academy of Sciences, Rostov on Don 344006, Russia

Received 31 January 2007; revised 4 June 2007; accepted 9 June 2007

ABSTRACT: The crown-ether functionalized 2-(*N*-acetyl-*N*-arylaminomethylene)benzo[*b*]thiophene-3(2*H*)-ones exhibit photochromic behavior involving photoinitiated *Z/E*-isomerization around the exocyclic C═C bond followed by a fast thermal N → O acetyl migration and syn → anti isomerization of the resulting kinetically stable *O*-acetyl isomers. The reverse rearrangement is an acid catalyzed reaction. The addition of alkali-earth metal ions to solutions of *N*-acyl isomers induces negligible changes in their UV/Vis spectra, which can be significantly enhanced after irradiation and conversion to the *O*-acyl isomers. The compounds obtained may be used as sensitive photodynamic chemosensors with the 'off-on' mechanism for alkali-earth ions (Ca^{2+}, Ba^{2+}). Quantum-chemical calculations using the DFT B3LYP/LanL2DZ method predict greater affinity of these sensors to Ca^{2+} ions (in the gas phase) and to Ba^{2+} ions (in acetonitrile). Copyright © 2007 John Wiley & Sons, Ltd.

KEYWORDS: photochromism; molecular switches; photodynamic chemosensors; quantum-chemical calculations; crown-ethers; ketoenamines; benzo[*b*]thiophene

INTRODUCTION

Photochromism is a reversible photoinduced transformation of a chemical species between two forms having different absorption spectra.[1–3] This transformation may be used for switching of various functions, one of which is associated with the ligating properties and is employed for the design of photodynamic and fluorogenic chemosensors for metal ions.[3,4] It has been recently shown that 2-(*N*-acyl-*N*-arylaminomethylene)benzo[*b*]-thiophene-, selenophene- and tellurophene-3(2*H*)-ones exhibit photochromic behavior allowing their application as solar-energy storage, chiroptical, and chemosensory systems.[5–7] Photochromism of these compounds is based on the mechanism involving a photoinitiated *Z/E*-isomerization around the exocyclic C═C bond followed by a fast thermal N → O acetyl migration and syn → anti isomerization of the resulting kinetically stable *O*-acetyl isomers.[6,8–12]

In this paper, we describe the synthesis of novel *N*-acylated crown-containing ketoenamines of the benzo[*b*]thiophene series and a spectral and quantum-chemical investigation into photoswitching of their complexation properties and sensing activity.

*Correspondence to: A. D. Dubonosov, Southern Scientific Center of Russian Academy of Sciences, 194/2 Stachka av., Rostov on Don, 344090, Russia.
E-mail: aled@ipoc.rsu.ru

RESULTS AND DISCUSSION

Synthesis

Crown-containing 2-(*N*-acetyl-*N*-arylaminomethylene)-benzo[*b*]thiophene-3(2*H*)-ones were obtained as previously described (Scheme 1).[5] The condensation of 3-hydroxybenzo[*b*]thiophene-2-carbaldehyde with the crown-ether substituted arylamines occurs smoothly to give ketoenamines **1a–c**. Heating the acetic anhydride solution of compounds **1a–c** in the presence of triethylamine affords *N*-acylated ketoenamines **2a–c** in 50–70% yields. The products of the photorearrangement of **3a–c** were prepared by the irradiation of acetonitrile solutions of **2a–c** in a quartz photo-reactor with unfiltered light of a high-pressure mercury lamp and subsequent evaporation of the solutions at ambient temperature.

The IR-spectra of *N*-acetyl isomers **2a–c** contain strong absorption bands of the amide (1690–1720 cm^{-1}) and exocyclic thiophene carbonyl groups (1660–1680 cm^{-1}). The initial *Z*-configuration of these compounds was confirmed by their ^1H NMR spectra that display characteristic downfield signals of the methine protons

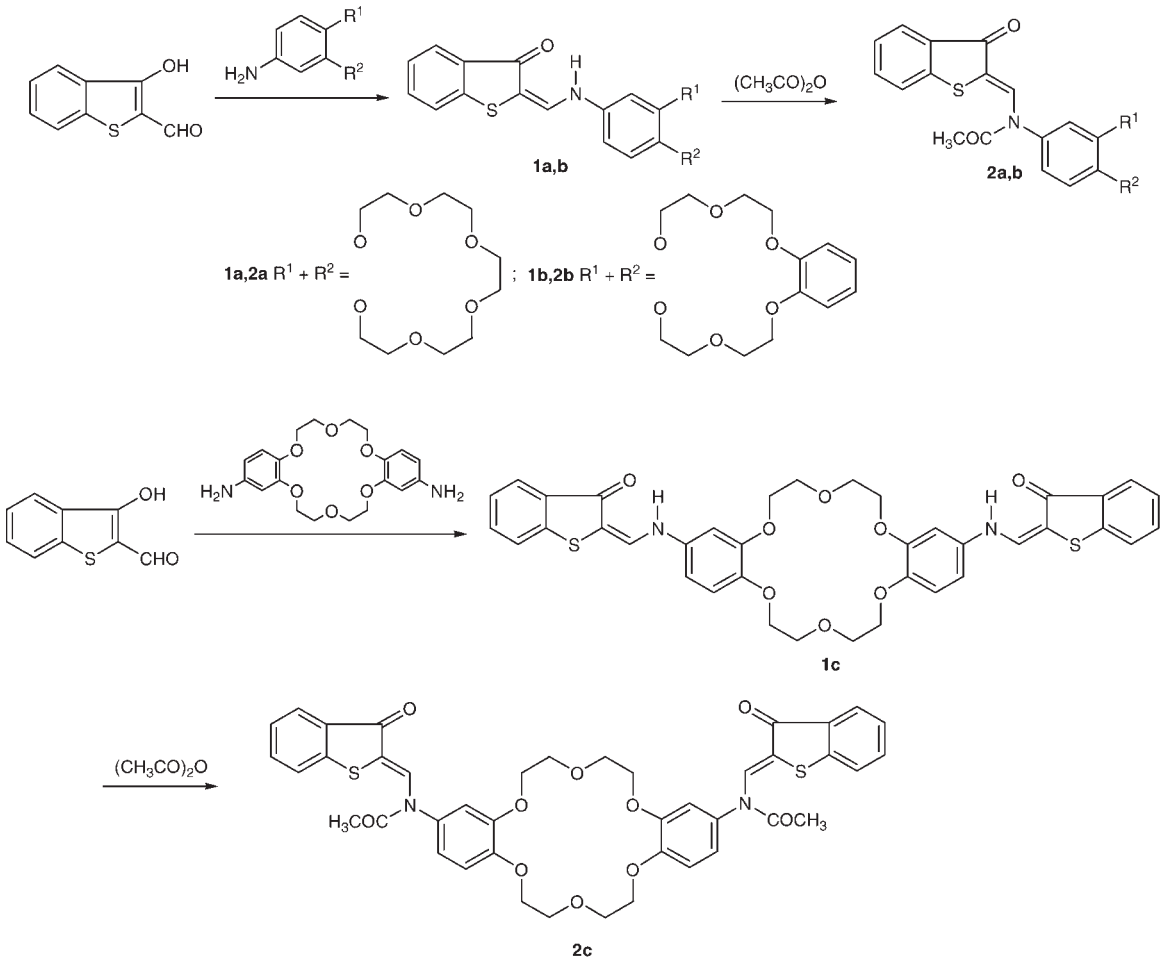

Scheme 1

at 8.75–8.90 ppm (whereas the signals of the methine protons of the *E*-isomers appear in the region of 5.90 ppm).[8,9]

Photochemistry

The absorption spectra of **2a–c** contain an intense long wavelength absorption band with λ_{max} at 428 nm (Table 1). Irradiation of acetonitrile solutions of **2a–c** at $\lambda = 436$ nm leads to a decrease in the long wavelength absorption accompanied by a simultaneous increase in the absorption at the shorter wavelength spectral region (λ_{max} at 370 nm) as shown in Figs 1 and 2. The spectral changes observed in Fig. 1 result from the photoinitiated *Z/E*-isomerization around the C=C double bond followed by a fast thermal N → O acetyl migration and syn → anti isomerization of the resulting kinetically stable *O*-acetyl isomers **3a,b**.[6] Compounds **3a,b** undergo *E/Z*-photoisomerization around the C=N bond at 273 K (λ_{irr} = 365 nm) followed by a fast thermal *Z/E*-process with entire restoration of the initial spectra (Fig. 3). For bis-*N,N′*-diacetyl compound **3c** only the total result of photoreaction is shown at Scheme 2. As seen from Fig. 2 the isosbestic point is not sharp as it is in the case of **2b**. Therefore we consider that the photochemical transformations of **3c** proceed as the stepwise process and include as intermediate the compound with one *O*-acetyl and one *N*-acetyl fragments. Overall quantum yields (φ) of the

Table 1. Spectral characteristics of **2,3** in acetonitrile solutions and quantum yields of the **2** → **3** rearrangement

Comp.	Absorption, λ_{max} (nm), ($\varepsilon \times 10^{-4}$, dm^3/mol/cm)	φ
2a	260 (2.12), 307 (1.70), 428 (1.08)	0.40 ± 0.01
2b	260 (2.04), 306 (1.66), 428 (1.04)	0.45 ± 0.01
2c	259 (4.16), 307 (3.44), 428 (2.12)	0.17 ± 0.005[a]
3a	308 (1.66), 370 (1.74)	—
3b	307 (1.60), 311 (1.82)	—
3c	309 (3.28), 370 (3.60)	—

[a] The overall quantum yield for stepwise rearrangement including transfers of both acetyl groups.

DOI: 10.1002/poc

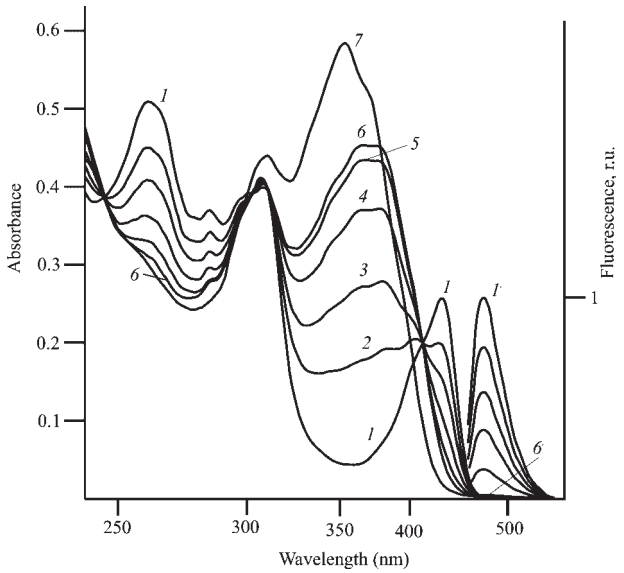

Figure 1. Absorption and emission spectra of **2b** in acetonitrile solution before irradiation (*1* and *1′*); after 5 s (*2* and *2′*); 10 s (*3* and *3′*); 20 s (*4* and *4′*); 40 s (*5* and *5′*); 120 s (*6* and *6′*) of irradiation ($\lambda_{irr} = 436$ nm, $C = 2.5 \times 10^{-5}$ M) and after addition of $Ba(ClO_4)_2$ (10-fold molar excess) (*7*)

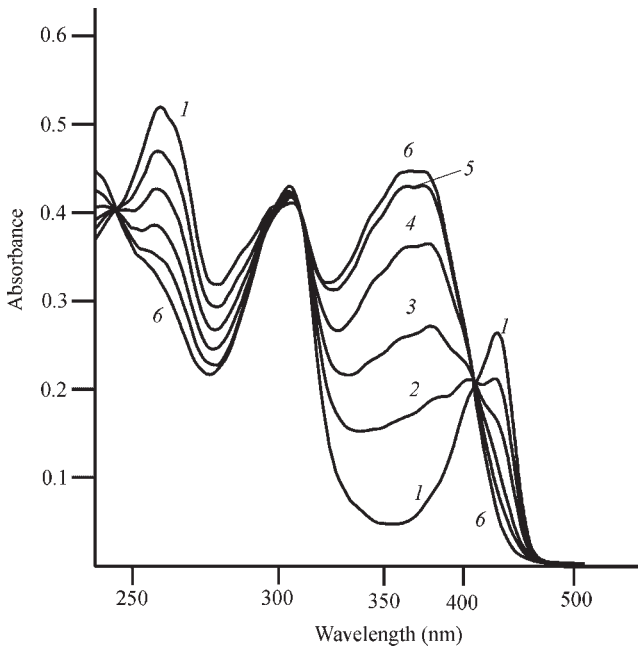

Figure 2. Absorption spectra of **2c** in acetonitrile solution before irradiation (*1*); after 5 s (*2*); 10 s (*3*); 20 s (*4*); 40 s (*5*); 120 s (*6*) of irradiation ($\lambda_{irr} = 436$ nm, $C = 1.25 \times 10^{-5}$ M)

2 → **3** photorearrangement are 0.40 (**2a**), 0.45 (**2b**), and 0.17 (**2c**).

The structures of compounds **3** were confirmed by their IR spectra containing the $\nu_{C=O}$ ester bands (1760–1770 cm^{-1}), by mass- and ^1H NMR spectra. At 293 K in acetonitrile, *N*-acylated ketoenamines **2** exhibit weak fluorescences with maxima at 460–470 nm which

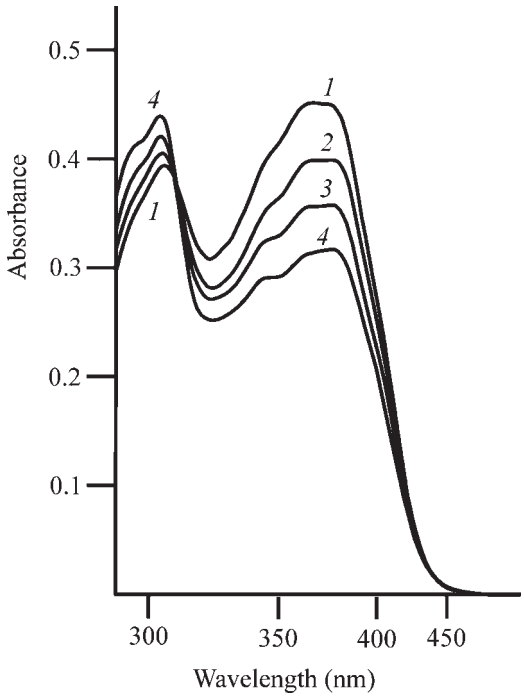

Figure 3. Absorption spectra of **2b** in acetonitrile solution at 273 K before irradiation (*1*) and after 1 min of the end of irradiation (*1*); after 2 s (*2*); 5 s (*3*); 15 s (*4*) of irradiation ($\lambda_{irr} = 365$ nm, $C = 2.5 \times 10^{-5}$ M)

disappear after the rearrangement into the *O*-acetyl isomers **3** due to the fast intersystem crossing processes ('on–off' process).[8,13] Fluorescence excitation and absorption spectra coincide. The thermal **3** → **2** back reaction occuring when passing a stream of dried HCl for 5–10 s through an acetonitrile solution of **3a–c**, leads to complete restoration of the initial absorption and emission spectra. The behavior of compounds **2** is typical of the systems displaying negative photochromism.[1]

Formation of metal complexes and switching the chemosensor properties

Addition of salts of alkali or alkali-earth metal ions (10-fold excess) to acetonitrile solutions of crown-containing 2-(*N*-acetyl-*N*-arylaminomethylene)benzo[*b*]-thiophene-3(2*H*)-ones **2a–c** induces very small changes in the UV spectra thus pointing to the negligible conjugation between crown-ether receptor and benzo[*b*]thiophene moieties in the *N*-acetyl form of the photochromic compounds (Scheme 3). In contrast, the photoinduced N → O acetyl rearrangement of **2a–c** occurring under irradiation of their acetonitrile solutions containing the metal salts results in substantial increase in the extinction of the long wavelength absorption band of *O*-acetyl ketoenamines **3a–c** ($\Delta\varepsilon$) accompanied by the blue shifts ($\Delta\lambda$) of that band ('off–on' switching of sensor activity) (Table 2, Fig. 4). The same spectral changes are

DOI: 10.1002/poc

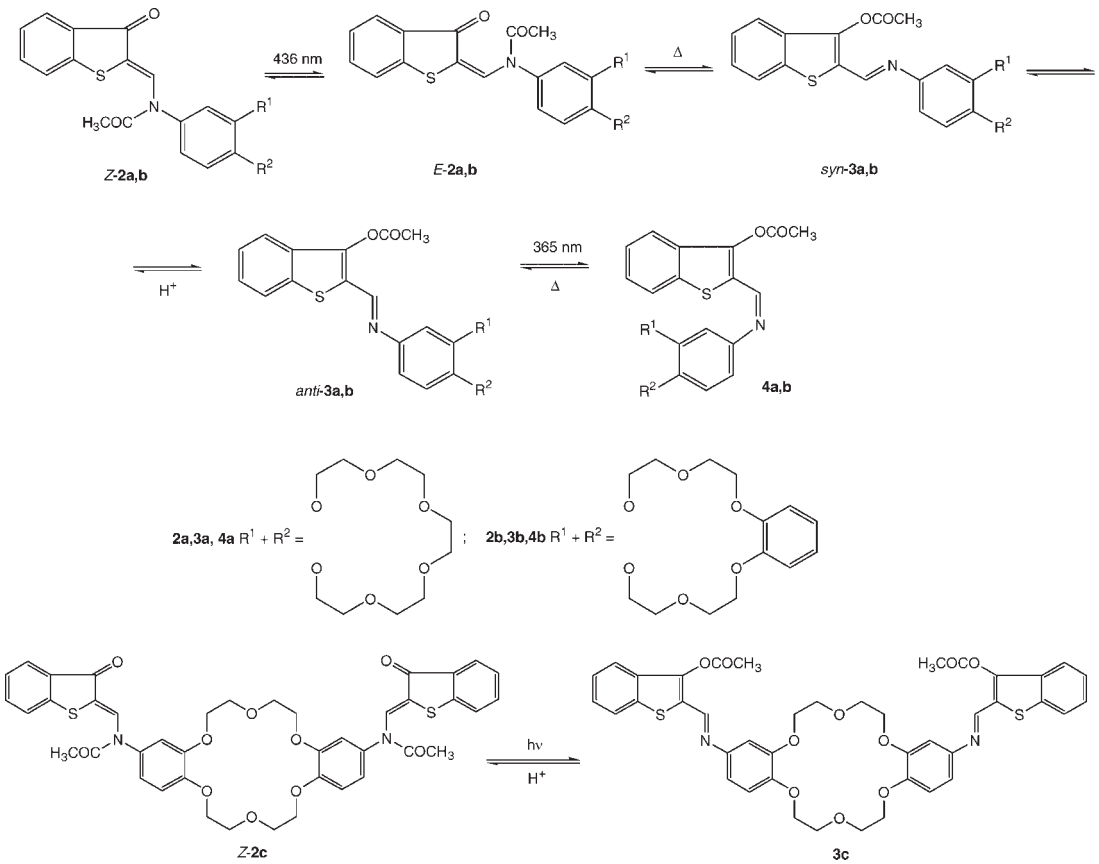

Scheme 2

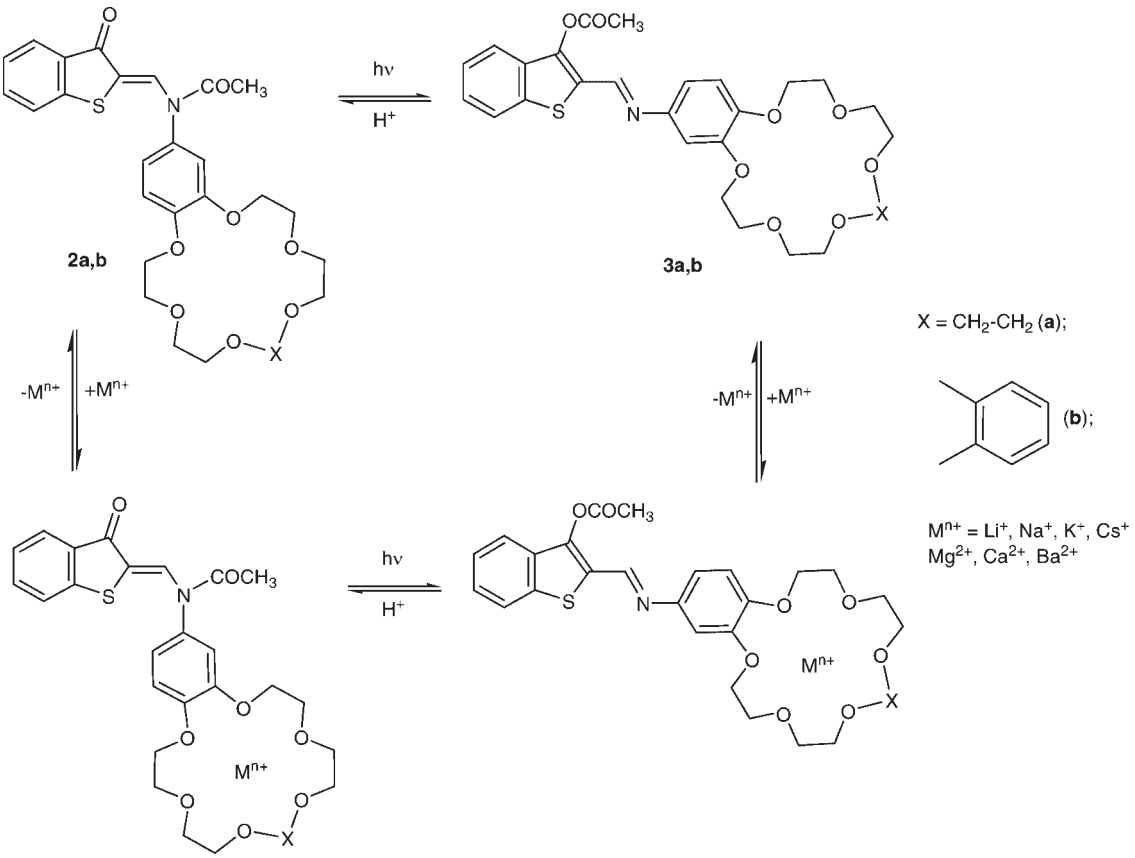

Scheme 3. (compounds **2a,b**)

DOI: 10.1002/poc

Table 2. Spectral changes in long-wave absorption band of complexes **3a–c**·M^{n+} as compared with **3a–c** and quantum yields of the **2a–c** → **3a–c** photorearrangements in acetonitrile in the presence of M^{n+}

	3	Li^+	Na^+	K^+	Cs^+	Mg^{2+}	Ca^{2+}	Ba^{2+}
a	$\Delta\varepsilon$, %	3.2	9.7	11.3	5.5	7.9	26.7	26.7
	$\Delta\lambda \pm 1$, nm	0	4	6	3	4	10	10
	$\varphi \pm 0.01$	0.40	0.57	0.56	0.49	0.51	0.57	0.64
b	$\Delta\varepsilon$, %	9.2	16.4	18.1	9.0	18.7	32.4	40.3
	$\Delta\lambda \pm 1$, nm	0	3	3	0	4	10	10
	$\varphi \pm 0.01$	0.43	0.54	0.62	0.46	0.53	0.62	0.69
c	$\Delta\varepsilon$, %	8.9	19.7	21.3	12.6	20.1	36.2	38.1
	$\Delta\lambda \pm 1$, nm	0	3	5	2	4	5	6
	$\varphi \pm 0.005$	0.16	0.19	0.20	0.15	0.17	0.21	0.22

also observed upon addition of the corresponding salts to solutions of photo-obtained *O*-isomers (Scheme 3).

Quantum yields of the photoreactions **2** → **3** in acetonitrile solutions containing metal ions are higher than those for the reactions in cation-free solution (Table 2). The alkaline-earth metal ions induce larger changes in the absorption spectra of the photoisomers **3** and provide for higher quantum yields of the **2** → **3** rearrangement compared with alkali metal ions. For **3a–c,** the greatest spectral response is observed for the case of Ca^{2+} and especially Ba^{2+} ions.

Complexation of **3a** with Ba^{2+} ions gives rise to appreciable downfield shifts of the proton signals in the ^1H NMR spectrum. This effect was the most pronounced for the crown-ether methylene protons close to the metal ion. With increase in the distance between the protons and the central metal ion, the downfield shifts gradually decrease (Table 3). This observation is a typical indication of metal ion incorporation to the crown-ether receptor.[14,15]

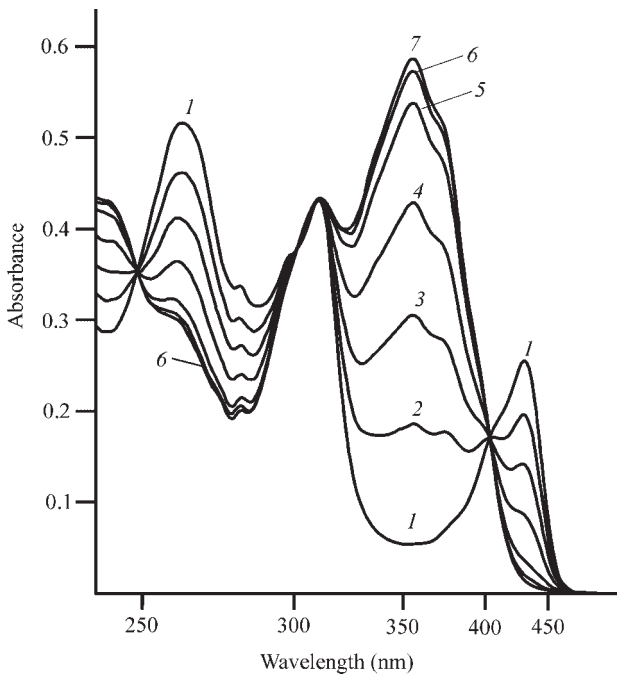

Figure 4. Absorption spectra of **2b**·Ba^{2+} in acetonitrile solution before irradiation (*1*); after 3 s (*2*); 6 s (*3*); 12 s (*4*); 24 s (*5*); 36 s (*6*); 72 s (*7*) of irradiation (λ_{irr} = 436 nm, $C_{2b} = 2.5 \times 10^{-5}$ M, $C_{Ba^{2+}} = 2.5 \times 10^{-4}$ M

The formation of complexes **3a–c** with Ca^{2+} and Ba^{2+} was also studied by spectrophotometric titration.[16] The mole ratio of **3** to metal ion was varied by adding aliquots of an acetonitrile solution containing certain concentration of metal ions to a solution of **3** in such a way that the concentration of **3** after mixing of two solutions remained constant (total volume 2×10^{-3} L). The absorption was monitored at a wavelength at which the metal–ligand complex absorbs ($\lambda = 350$ nm). The mole-ratio plots obtained pointed to the formation of Ca^{2+} and Ba^{2+} complexes of 1:1 stoichiometries (Figs 5 and 6). The stability constants of the complexes are listed in Table 4.

Quantum-chemical calculations

In order to analyze the factors which influence crown specificity quantum-chemical calculations using the DFT B3LYP/LanL2DZ method were carried out.[17] 4-Aminobenzo-18-crown-6 **5** was selected as the model system.

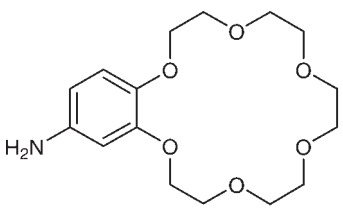

5

According to the calculations, conformational isomers of compound **5** are in close energetic proximity. The lowest energy structure **5a** is shown in Fig. 7 . Other less stable conformers are destabilized relative to **5a** by

DOI: 10.1002/poc

Table 3. ^{1}H NMR data for **2,3a** before and after addition of Ba^{2+} (CD_3CN, δ, ppm)

	CH_3	6–CH_2O	2–CH_2O	2–CH_2O	Ar	=CH
2a	2.04 s (3H)	3.51–3.66 m (12H)	3.68–3.83 m (4H)	4.09–4.30 m (4H)	6.94–7.10 m (3H) 7.22–7.81 m (4H)	8.80 s (1H)
2a·Ba^{2+}	2.07 s (3H)	3.74–3.93 m (12H)	3.95–4.06 m (4H)	4.26–4.46 m (4H)	7.10–7.82 m (7H)	8.79 s (1H)
3a	2.47 s (3H)	3.48–3.64 m (12H)	3.71–3.82 m (4H)	4.13–4.25 m (4H)	6.89–7.00 m (3H) 7.41–7.95 m (4H)	8.78 s (1H)
3a·Ba^{2+}	2.49 s (3H)	3.76–3.90 m (12H)	3.97–4.03 m (4H)	4.31–4.42 m (4H)	7.01–7.14 m (3H) 7.43–7.94 m (4H)	8.79 s (1H)

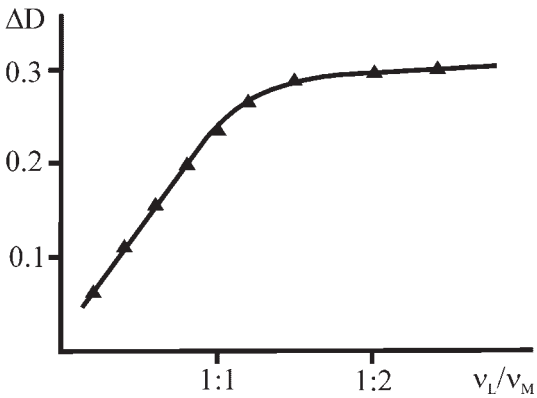

Figure 5. Mole-ratio plots for the complex of **2b** with $Ca(ClO_4)_2$ in acetonitrile solution; $C_M = 5 \times 10^{-5}$ M (const); ($\lambda_{obs} = 350$ nm)

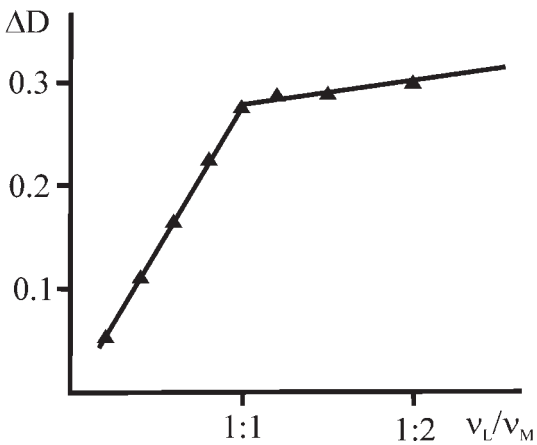

Figure 6. Mole-ratio plots for the complex of **2b** with $Ba(ClO_4)_2$ in acetonitrile solution; $C_M = 5 \times 10^{-5}$ M (const); ($\lambda_{obs} = 350$ nm)

2–9 kcal/mol. The calculated macrocyclic ring structure of 4-aminobenzo-18-crown-6 was found to be asymmetric with unequal O···O distances. Interaction of aminobenzo-18-crown-6 conformers with Ca^{2+} or Ba^{2+} ions leads to the formation of a number of metal

Table 4. Stability constants of the complexes of **3a–c** with the Ca^{2+} and Ba^{2+} cations in MeCN

	lg *K*	
3	Ca^{2+}	Ba^{2+}
a	5.55 ± 0.1	7.03 ± 0.1
b	5.67 ± 0.15	7.20 ± 0.1
c	5.40 ± 0.1	7.32 ± 0.15

complexes that differ slightly in their relative stability. The complexes of **5a** with calcium and barium ions are presented in Fig. 8. The formation of the cations **6** is accompanied by appreciable compression of the crown-ether cavity. The benzene ring in **5** increases the rigidity of the macrocycle, reduces the size of the crown-ether cavity, and provides favorable steric conditions for the coordination of metal ions. In the case of the Ca^{2+} complex, the shortening of the O···O distances as compared with the free ligand is equal to 0.1–1.0 Å (on average 0.44 Å). The calculated Ca···O bond lengths are nearly equivalent and are 2.43–2.48 Å. The Ba^{2+} ion size better fits into the macrocycle cavity of **5** and the conformation of barium complex is virtually planar. The calculated Ba···O bond lengths are in the range of 2.73–2.81 Å. For the Ba^{2+} complex, compression of the macrocycle cavity is less pronounced compared to the Ca^{2+} complex: the interatomic O···O distances are shortened by ~0.35 Å. Energies of binding (E_{bind}) of complexes **6** (calculated as the difference between total energies of **5** and the sum of energies of the isolated monomer **5a** and M^{2+}) are equal to 256.1 (M = Ca) and 194.7 (M = Ba) kcal/mol. The gas phase binding affinity of **5** decreases with increase in the cation size; this observation is in agreement with previous results on alkali metal complexes.[18–21] Thus, in spite of more favorable steric conditions for the complexation of the barium cation, the complex of **5a** with Ca^{2+} is characterized by a higher E_{bind} value. This result is in conflict with the 'hole-size' concept.[22]

DOI: 10.1002/poc

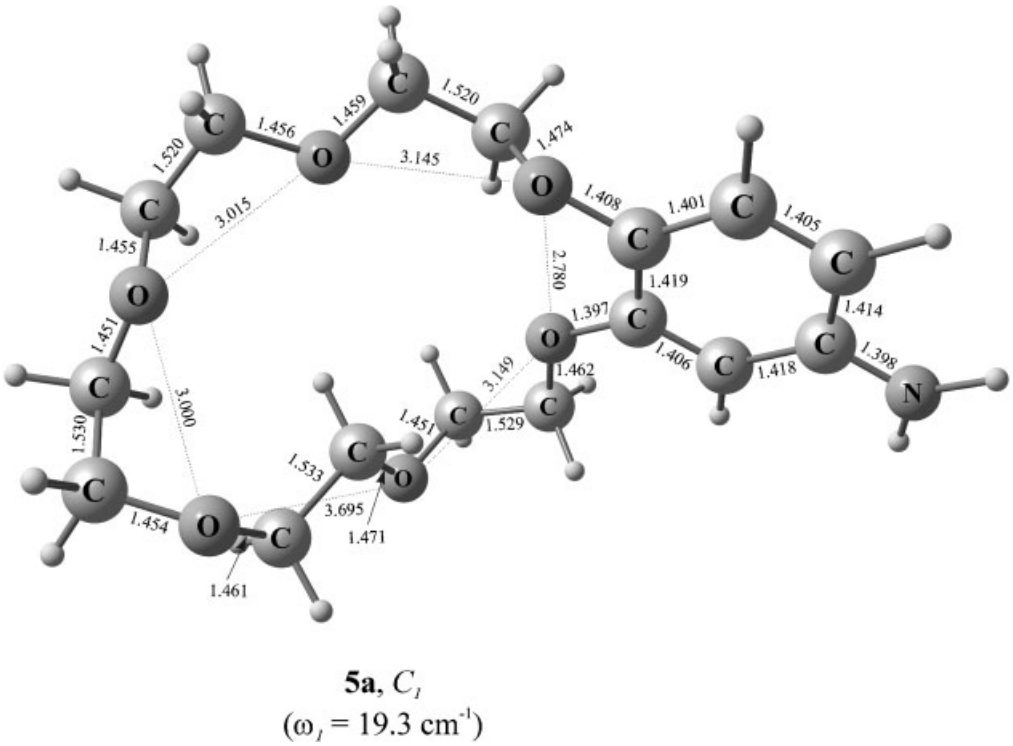

Figure 7. Structural characteristics and values of the lowest harmonic vibration frequencies of the lowest-energy conformer **5a** of aminobenzo-18-crown-6 corresponding to the energy minima calculated by B3LYP/LanL2DZ method. Bond lengths are given in angström units

The electronic structure of complexes **5** has been analyzed using the NBO (natural bond orbital)-scheme.[23] According to the NBO-analysis, the principal attractive component of binding in complexes **5** is due to donation of electron density from orbitals of the crown oxygen lone pairs to empty s-orbitals of the metal ion. The calculations predict a decrease in the $n_O \rightarrow \sigma^{2+}_M$ orbital interaction energies on passing from calcium to barium complex (33 and 12 kcal/mol, respectively) that correlates with lowering E_{bind} and charge transfer from crown-ether to cation (0.42 and 0.27 e, for calcium and barium complexes, respectively). These effects are due to the increase in the energy gap between interacting orbitals of the fragments. Thus, in the gas-phase aminobenzo-18-crown-6 **5** is characterized by greater affinity with respect to Ca^{2+} as compared to Ba^{2+}. This selectivity is governed mainly by the orbital effects as compared to the influence of the steric factors.

The quantum-chemical calculations showed that the interaction of cations with solvent molecules may lead to significant changes in crown specificity.[19,20] The crown selectivity in solution is determined by a balance between the energies of crown-cation interaction and cation solvation. In this work, the influence of specific solvation on selectivity of **5** was examined for the case of acetonitrile.

The solvent effect is estimated based on evaluation of energetics of the process in which some solvent molecules in the coordination shell of the metal cation are replaced by the crown-ether. This approach has been found to be quite reliable and has been applied for the evaluation of selectivity of various crown complexes.[19,20] The exchange reaction (1) may serve as an appropriate measure of selectivity of crown-ether in solution.

$$\mathrm{Ca}^{2+} \cdot (\mathrm{MeCN})_n + 5(\mathrm{M} = \mathrm{Ba}) \rightarrow \mathrm{Ba}^{2+} \cdot (\mathrm{MeCN})_n + 5(\mathrm{M} = \mathrm{Ca}) + \Delta E_1 \quad (1)$$

According to calculations of binding energies performed for Ca^{2+} and Ba^{2+} solvate complexes (Fig. 9), the calcium ion is characterized by a higher affinity to acetonitrile than the barium ion (Table 5). Beginning from solvates with $n = 5$ interaction of a cation M^{2+} with solvent becomes energy preferred than that with crown-ether. This effect is more pronounced for calcium. Whereas no noticeable selectivity is detected for solvates with low n values ($n = 4$, 5) the rise in n reveals for the crown selectivity with respect to barium in accordance with our experimental data.

The coordination sphere of cation in crown complexes may be enlarged through additional coordination of solvent molecules.[20] Thus, addition of four acetonitrile molecules to complexes **6** leads to the formation of complexes **10** (Fig. 10). As can be seen from Fig. 6, the additional coordination is accompanied by significant

DOI: 10.1002/poc

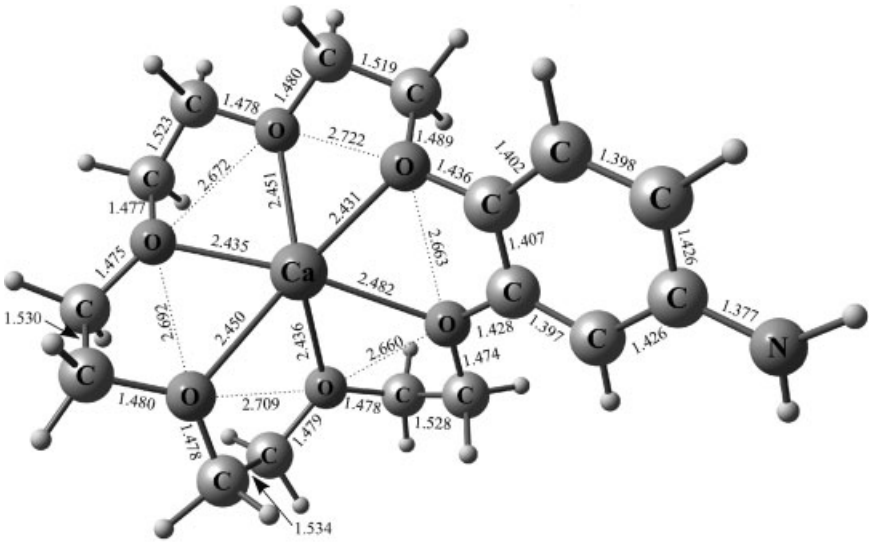

6 (M = Ca)
(ω_1 = 26.0 cm^{-1})

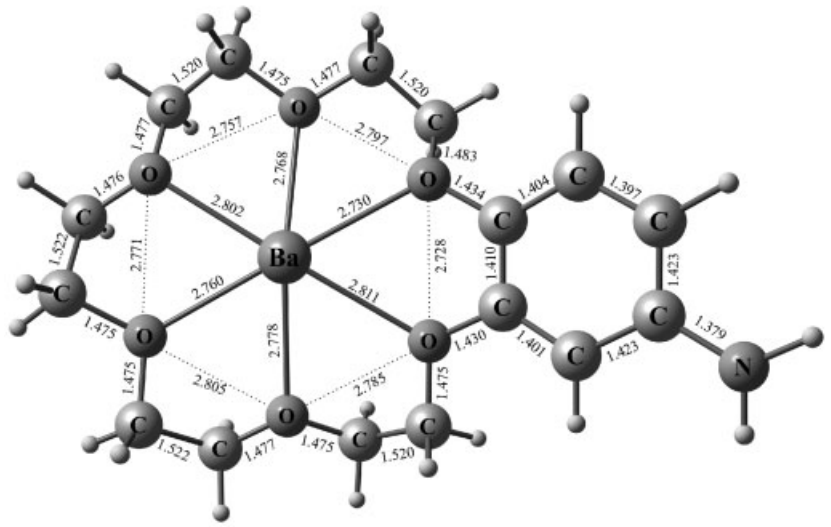

6 (M = Ba)
(ω_1 = 24.3 cm^{-1})

Figure 8. Structural characteristics and values of the lowest harmonic vibration frequencies of complexes **6** (M = Ca, Ba) corresponding to the energy minima calculated by B3LYP/LanL2DZ method. Bond lengths are given in angström units

weakening of the crown-cation M···O bonds. At the same time, the systems **90** are stable with respect to dissociation of free crown-ether **5a** and solvated cation **7** (reaction 2). The barium complex is characterized by greater stability in this respect ($\Delta E_2 = -79.1$ kcal/mol for Ca and -87.3 kcal/mol for Ba).

$$10 \rightarrow \mathbf{5a} + 7 + \Delta E_2 \qquad (2)$$

The above quantum-chemical calculations coincide with available theoretical data on the dependence of crown-ether selectivities on the solvent.[19–21]

CONCLUSIONS

The crown-ether functionalized 2-(*N*-acetyl-*N*-arylaminomethylene)benzo[*b*]thiophene-3(2*H*)-ones **2a–c** represent a new type of molecular switches with the «off–on» mechanism displaying the chemosensor activity for Ca^{2+} and especially Ba^{2+} (in parallel with 'on–off' mechanism of fluorescence activity) caused by the photoinitiated *Z/E*-photoisomerization followed by a fast thermal N → O acetyl migration and syn → anti isomerization of the resulting kinetically stable *O*-acetyl isomers. The DFT B3LYP/LanL2DZ quantum-chemical

DOI: 10.1002/poc

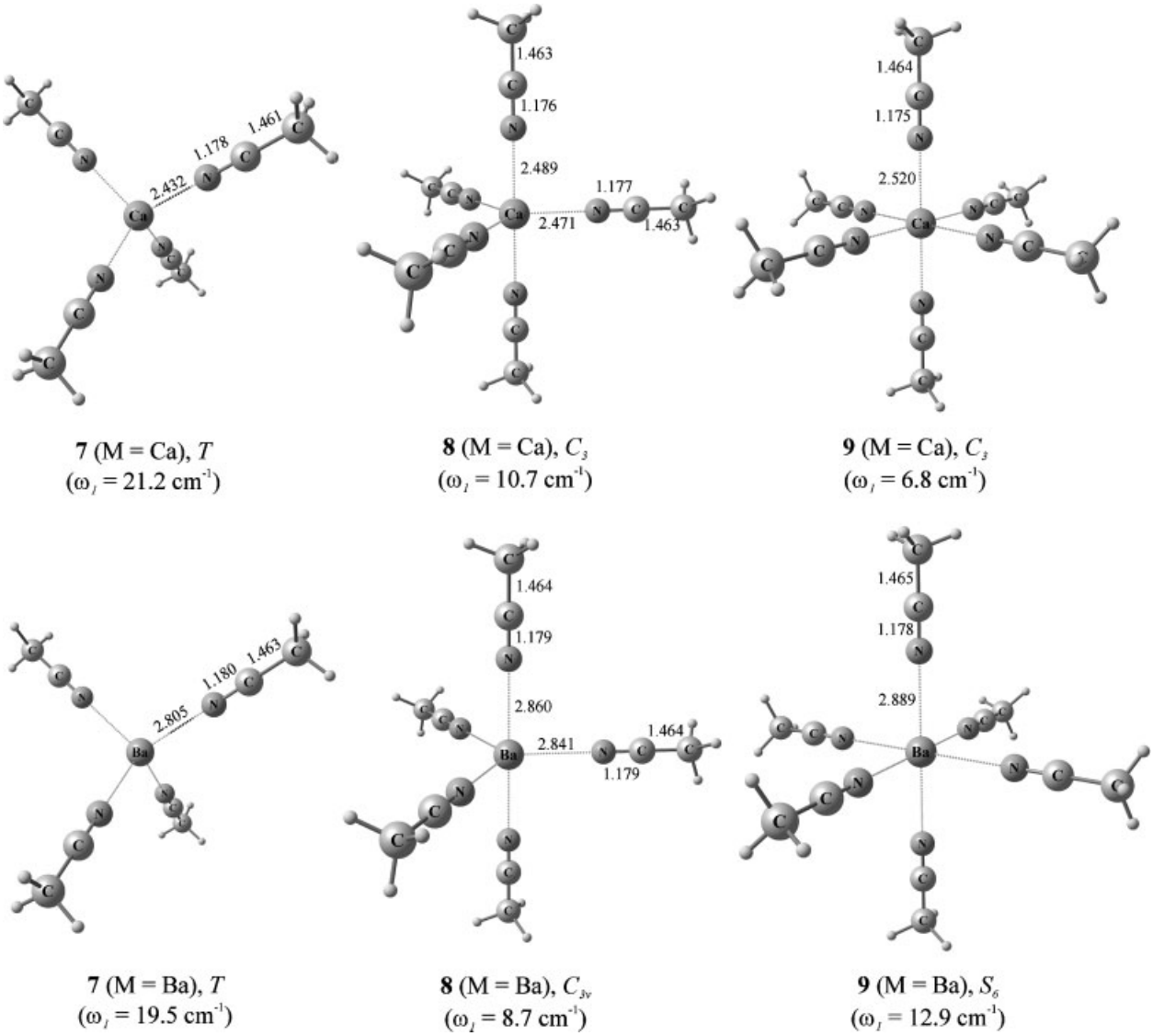

7 (M = Ca), T ($\omega_1 = 21.2\ cm^{-1}$)
8 (M = Ca), C_3 ($\omega_1 = 10.7\ cm^{-1}$)
9 (M = Ca), C_3 ($\omega_1 = 6.8\ cm^{-1}$)
7 (M = Ba), T ($\omega_1 = 19.5\ cm^{-1}$)
8 (M = Ba), C_{3v} ($\omega_1 = 8.7\ cm^{-1}$)
9 (M = Ba), S_6 ($\omega_1 = 12.9\ cm^{-1}$)

Figure 9. Structural characteristics and values of the lowest harmonic vibration frequencies of solvated complexes $[M^{2+}\cdot(MeCN)_n]$, (M = Ca, Ba; $n = 4$–6) corresponding to the energy minima calculated by the B3LYP/LanL2DZ method. Bond lengths are given in angström units

calculations predict the greater affinity of 4-aminobenzo-18-crown-6 derivatives **2** to Ca^{2+} in the gas phase; in acetonitrile solution, their relative sensitivity inverts and the formation of Ba^{2+} complexes becomes more preferable.

Table 5. Binding energies[a] (E_{bind}) of complexes $[M^{2+}\cdot(MeCN)_n]$, (M = Ca, Ba; $n = 4$–6) and reaction energies (ΔE_1 in) for the exchange reactions (1) calculated by B3LYP/LanL2DZ method

	E_{bind}, kcal/mol		
n	M = Ca	M = Ba	ΔE_1, kcal/mol
4	243.5	183.8	1.6
5	276.6	211.7	−3.5
6	306.8	236.9	−8.6

[a] Calculated as difference between total energies of $[M^{2+}\cdot(MeCN)_n]$ complex and the sum of energies of the isolated monomers.

EXPERIMENTAL

General

^{1}H NMR spectra were recorded on a Varian Unity 300 spectrometer; δ values and spin–spin coupling constants were measured within 0.01 ppm and 0.1 Hz, respectively. IR spectra in Nujol were measured using a Specord 75IR spectrometer. UV-Vis absorption spectra in CH_3CN were obtained with a Specord M-40 spectrophotometer. Fluorescence emission and excitation spectra were recorded on a Hitachi 650-60 spectrofluorimeter. Irradia-

DOI: 10.1002/poc

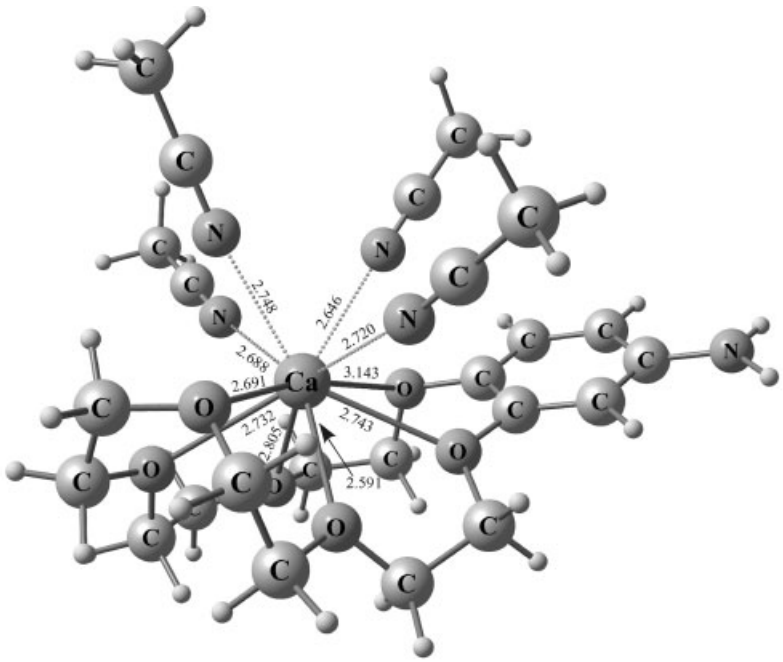

10 (M = Ca)
(ω_i = 14.5 cm^{-1})

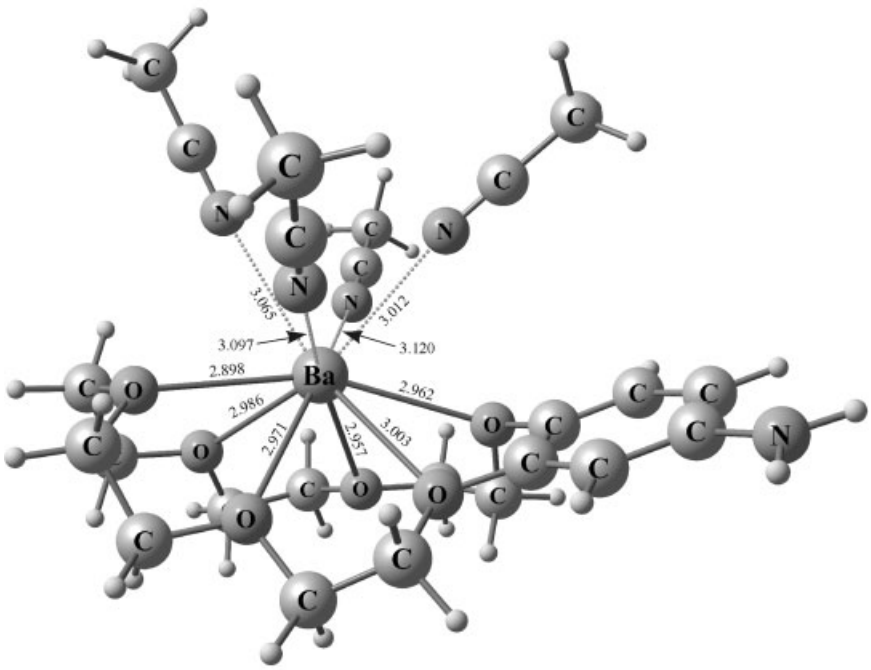

10 (M = Ba)
(ω_i = 9.0 cm^{-1})

Figure 10. Structural characteristics and values of the lowest harmonic vibration frequencies of complexes **10** corresponding to the energy minima calculated by the B3LYP/LanL2DZ method. Bond lengths are given in angström units

tion of solutions ($V = 2 \times 10^{-3}$ L) was carried out by filtered light of a high-pressure mercury lamp DRSh (250 W) supplied with a set of glass filters ($\lambda_{irr} = 436$ nm). The intensity of light used for irradiation of the solutions was 3×10^{16} photons/s for the spectral line 436 nm. Alkali metal ions were added to solutions as iodides and alkali-earth metal ions—as perchlorates. Potassium ferrioxalate was used as the actinometer for the

DOI: 10.1002/poc

determination of quantum yields (φ) of the photoreactions.[24] The samples had absorbance of 0.95 at $\lambda_{irr} = 436$ nm ($l = 1$ cm, $V = 2 \times 10^{-3}$ L, rate of conversion of $2 \rightarrow 3 \leq 5\%$, the experimental error in φ is $\pm$ 5%). The stability constants of the complexes were determined as previously described.[25] Mass spectra were recorded on MX-1321A and Finnigan LCQ Deca XP MAX spectrometers.

2-[(6,7,9,10,12,13,15,16,18,19-Decahydro-5,8,11,14,17,20-hexaoxabenzocyclooctadecen-2-ylamino)methylene]-benzo[b]thiophene-3(2H)-one (**1a**). A solution of 4-aminobenzo-18-crown-6 (1.8 g, 5.5 mmol) in 3 mL of acetonitrile was added to a solution of 3-hydroxybenzo[*b*]thiophene-2-carbaldehyde (0.98 g, 5.5 mmol) and refluxed for 3–5 min. The precipitate was filtered and crystallized from toluene to give **1a** as a red powder. Yield 75%; m.p. 113–115°C. IR (nujol): ν (cm^{-1}) 1630, 1600, 1585, 1565, 1510. ^{1}H NMR (300 MHz, DMSO-d_6), δ 3.50–4.21 (m, 20H, 10CH_2O), 6.89–7.10 (m, 7H, Ar-H), 8.20 (d, $J = 13.7$ Hz, 1H, =CH), 9.84 (d, $J = 13.7$ Hz, 1H, NH) ppm. MS (EI): *m/z* 487 $[M]^+$. Anal. Calcd for $C_{25}H_{29}NO_7S$, C 61.59, H 6.00, N 2.87; found, C 61.43, H 6.11, N 2.80%.

2-[(6,7,9,10,17,18,20,21-Octahydro-5,8,11,16,19,22-hexaoxadibenzo[a,j]cyclooctadecen-2-ylamino)methylene]benzo[b]thiophene-3(2H)-one (**1b**) was synthesized in a similar way as **1a** and crystallized from toluene-DMFA mixture (1:1). Yield of a red powder 90%, mp 207–209°C. IR (nujol): ν (cm^{-1}) 1640, 1595, 1570, 1505. ^{1}H NMR (300 MHz, DMSO-d_6), δ 3.82–4.24 (m, 16H, 8CH_2O), 6.78–7.84 (m, 11H, Ar-H), 8.23 (d, $J = 13.6$ Hz, 1H, =CH), 9.85 (d, $J = 13.6$ Hz, 1H, NH) ppm. MS (EI): *m/z* 535 $[M]^+$. Anal. Calcd for $C_{29}H_{29}NO_7S$, C 65.03, H 5.46, N 2.62; found, C 64.95, H 5.60, N 2.51%.

N,N′-Bis(3-oxo-3H-benzo[b]thiophene-2-ylidenemethyl)-6,7,9,10,17,18,20,21-octahydro-5,8,11,16,19,22-hexaoxadibenzo[a,j]cyclooctadecen-2,14-diamine (**1c**) was synthesized in a similar way as **1a** (from 5.5 mmol of 4,4′-diaminodibenzo-18-crown-6 and 11 mmol of 3-hydroxybenzo[*b*]thiophene-2-carboxaldehyde) and crystallized from DMFA. Yield of a red powder 85%, mp 304–306°C. IR (nujol): ν (cm^{-1}) 1665, 1600, 1545. ^{1}H NMR (300 MHz, DMSO-d_6), δ 3.76–4.21 (m, 16H, 8CH_2O), 6.82-7.83 (m, 14H, Ar-H), 8.25 (d, $J = 13.4$ Hz, 2H, =CH), 10.02 (d, $J = 13.4$ Hz, 2H, NH) ppm. MS (EI): *m/z* 710 $[M]^+$. Anal. Calcd for $C_{38}H_{34}N_2O_8S_2$, C 64.21, H 4.82, N 3.94; found, C 64.11; H 4.73; N 3.81%.

2-{[N-Acetyl-(6,7,9,10,12,13,15,16,18,19-decahydro-5,8,11,14,17,20-hexaoxabenzocyclooctadecen-2-yl)amino]-methylene}benzo[b]thiophene-3(2H)-one (**2a**). Compound **1a** (0.3 g, 0.6 mmol) was dissolved in acetic anhydride (1 mL) in the presence of triethylamine and refluxed for 10 min. The precipitate was filtered and crystallized from toluene. Yield of yellow crystals 68%, mp 160–161°C. IR (nujol): ν (cm^{-1}) 1690, 1660, 1580, 1550, 1500. ^{1}H NMR (300 MHz, DMSO-d_6), δ 2.04 (s, 3H, CH_3), 3.63–4.22 (m, 20H, 10CH_2O), 6.89–7.76 (m, 7H, Ar-H), 8.75 (s, 1H, =CH) ppm. MS (EI): m/z 529 $[M]^+$. Anal. Calcd for $C_{27}H_{31}NO_8S$, C 61.23, H 5.90, N 2.64; found, C 61.32, H 5.84, N 2.60%.

2-{[N-Acetyl-(6,7,9,10,17,18,20,21-octahydro-5,8,11,16,19,22-hexaoxadibenzo[a,j]cyclooctadecen-2-yl)amino]-methylene}benzo[b]thiophene-3(2H)-one (**2b**) was synthesized in a similar way as **2a** and crystallized from toluene. Yield of a yellow powder 74%, mp 210–212°C. IR (nujol): ν (cm^{-1}) 1705, 1675, 1590, 1565, 1515. ^{1}H NMR (300 MHz, DMSO-d_6), δ 2.08 (s, 3H, CH_3), 4.00–4.36 (m, 16H, 8CH_2O), 6.76–7.84 (m, 11H, Ar-H), 8.90 (s, 1H, =CH) ppm. MS (EI): *m/z* 577 $[M]^+$. Anal. Calcd for $C_{31}H_{31}NO_8S$, C 64.46, H 5.41, N 2.42; found, C 64.32, H 5.29, N 2.34%.

N, N′-Bis(3-oxo-3H-benzo[b]thiophene-2-ylidenemethyl)-N,N′-diacetyl-6,7,9,10,17,18,20,21-octahydro-5,8,11,16,19,22-hexaoxadibenzo[a,j]cyclooctadecen-2,14-diamine (**2c**) was synthesized in a similar way to **2a** and crystallized from DMFA. Yield of a yellow powder 52%, mp 289–291°C. IR (nujol): ν (cm^{-1}) 1715, 1690, 1600, 1575, 1520. ^{1}H NMR (300 MHz, DMSO-d_6), δ 2.00 (s, 6H, 2CH_3), 3.64–4.22 (m, 16H, 8CH_2O), 7.04–7.74 (m, 14H, Ar-H), 8.78 (s, 2H, =CH) ppm. MS (EI): m/z 794 $[M]^+$. Anal. Calcd for $C_{42}H_{38}N_2O_{10}S_2$, C 63.46, H 4.82, N 3.52; found, C 63.29, H 4.71, N 3.60%.

2-[(6,7,9,10,12,13,15,16,18,19-Decahydro-5,8,11,14,17,20-hexaoxabenzocyclooctadecen-2-ylimino)methyl]-benzo[b]thiophene-3(2H)-yl acetate (**3a**). A solution of **2a** (0.3 g, 0.6 mmol) in 10 mL of acetonitrile was irradiated with a non-filtered light of a high-pressure mercury lamp for 2 h in quartz photo-reactor. Evaporation of this solution at ambient temperature affords **3a** as a yellow powder. Yield 100%, mp 66–67°C. IR (nujol): ν (cm^{-1}) 1770, 1610, 1580, 1510. ^{1}H NMR (300 MHz, CD_3CN), δ 2.46 (s, 3H, CH_3), 3.48–4.23 (m, 20H, 10CH_2O), 6.88–7.92 (m, 7H, Ar-H), 8.78 (s, 1H, =CH) ppm. MS (EI): *m/z* 529 $[M]^+$. Anal. Calcd for $C_{27}H_{31}NO_8S$, C 61.23, H 5.90, N 2.64; found, C 61.20, H 5.85, N 2.71%.

2-[(6,7,9,10,17,18,20,21-Octahydro-5,8,11,16,19,22-hexaoxadibenzo[a,j]cyclooctadecen-2-ylimino)methyl]-benzo[b]thiophene-3(2H)-yl acetate (**3b**) was synthesized in a similar way to **3a**.Yield of a yellow powder 100%, mp 104–105°C. IR (nujol): ν (cm^{-1}) 1760, 1610, 1570, 1500. ^{1}H NMR (300 MHz, DMSO-d_6), δ 2.53 (s, 3H, CH_3), 3.84–4.22 (m, 16H, 8CH_2O), 6.80–7.87 (m, 11H, Ar-H), 8.77 (s, 1H, =CH) ppm. MS (EI): *m/z* 577 $[M]^+$. Anal. Calcd for $C_{31}H_{31}NO_8S$, C 64.46, H 5.41, N 2.42; found, C 64.37, H 5.40, N 2.54%.

N,N′-Bis(3-acetoxybenzo[b]thiophene-2-ylmethylene)-6,7,9,10,17,18,20,21-octahydro-5,8,11,16,19,22-hexaoxadibenzo[a,j]cyclooctadecen-2,14-diamine (**3c**) was synthesized in a similar way to **3a**.Yield of a yellow powder 100%, mp 164–165°C. IR (nujol): ν (cm^{-1}) 1770, 1610, 1580, 1500. ^{1}H NMR (300 MHz, DMSO-d_6), δ 2.49 (s, 6H, 2CH_3), 3.83–4.22 (m, 16H, 8CH_2O), 6.84–7.85 (m, 14H, Ar-H), 8.77 (c, 2H, =CH) ppm. MS (EI): m/z 794

DOI: 10.1002/poc

$[M]^+$. Anal. Calcd for $C_{42}H_{38}N_2O_{10}S_2$, C 63.30, H 4.91, N 3.50; found, C 63.30, H 4.91, N 3.50%.

Acknowledgements

This work was supported by Russian Foundation for Basic Research (06-03-32561, 05-03-32470), Ministry of Education and Science of Russian Federation (RNP 2.2.2.2.5592, RNP 2.1.1.4939) and President's of Russian Federation grant (NSh-4849.2006.3) and President's of Russian Federation grant.

REFERENCES

1. Bouas-Laurent H, Durr H. *Pure Appl. Chem.* 2001; **73**: 639–665.
2. Durr H, Bouas-Laurent H (eds). *Photochromism*. Elsevier: Amsterdam, 2003.
3. Crano JC, Guglielmetti R (eds). *Organic Photochromic and Thermochromic Compounds*. Kluwer Academic/Plenum Publishers: New York, vol. **1**, 1998 and vol. 2, 1999.
4. Chernyshev AV, Voloshin NA, Raskita IM, Metelitsa AV, Minkin VI. *J. Photochem. Photobiol. A.* 2006; **184**: 289–297.
5. Dubonosov AD, Minkin VI, Bren VA, Popova LL, Rybalkin VP, Shepelenko EN, Tkalina NT, Tsukanov AV. *Arch. Org. Chem. (ARKIVOC).* 2003; **13**: 12–20.
6. Bren VA, Dubonosov AD, Popova LL, Rybalkin VP, Sadekov ID, Shepelenko EN, Tsukanov AV. *Arch. Org. Chem. (ARKIVOC).* 2005; **7**: 60–66.
7. Bren VA, Dubonosov AD, Minkin VI, Gribanova TN, Rybalkin VP, Shepelenko EN, Tsukanov AV, Borisenko RN. *Mol. Cryst. Liq. Cryst.* 2005; **431**: 417–422.
8. Minkin VI, Bren VA, Lyubarskaya AE. In *Organic Photochromes*, Eltsov AV (ed). Consultants Bureau: New York and London, 1990; Chapter. 5: 218–244.
9. Aldoshin SM, Dyachenko OA, Atovmyan LO, Minkin VI, Bren VA, Paluy GD. *Z. Kristallogr.* 1982; **159**: 143–159.
10. Bren VA, Minkin VI, Dubonosov AD, Chernoivanov VA, Rybalkin VP, Borodkin GS. *Mol. Cryst. Liq. Cryst.* 1997; **297**: 247–253.
11. Dubonosov AD, Rybalkin VP, Vorob'eva YaYu, Bren VA, Minkin VI, Aldoshin SM, Tkachev VV, Tsukanov AV. *Russ. Chem. Bull., Int. Ed.* 2004; **53**: 2248–2252.
12. Rybalkin VP, Vorob'eva YaYu, Borodkin GS, Dubonosov AD, Tsukanov AV, Tkachev VV, Aldoshin SM, Bren VA, Minkin VI. *Russ. Chem. Bull., Int. Ed.* 2005; **54**: 2783–2789.
13. Knyazhanskii MI, Stryukov MB, Minkin VI, Lyubarskaya AE, Olekhnovich LP. *Bull. Russ. Acad. Sci., Physics.* 1972; **36**: 1102–1105.
14. Gromov SP, Ushakov EN, Fedorova OA, Baskin II, Buevich AV, Andryukhina EN, Alfimov MV, Johnels D, Edlund UG, Whitesell JK, Fox MA. *J. Org. Chem.* 2003; **68**: 6115–6125.
15. Kim Y-H, Hong J-I. *Chem. Commun.* 2002; 512–513.
16. Gans P, Sabatini A, Vacca A. *Talanta.* 1996; **43**: 1739–1742.
17. Frisch MJ, Trucks GW, Schlegel HB, Scuseria GE, Robb MA, Cheeseman JR, Montgomery JA, Jr, Vreven T, Kudin KN, Burant JC, Millam JM, Iyengar SS, Tomasi J, Barone V, Mennucci B, Cossi M, Scalmani G, Rega N, Petersson GA, Nakatsuji H, Hada M, Ehara M, Toyota K, Fukuda R, Hasegawa J, Ishida M, Nakajima T, Honda Y, Kitao O, Nakai H, Klene M, Li X, Knox JE, Hratchian HP, Cross JB, Adamo C, Jaramillo J, Gomperts R, Stratmann RE, Yazyev O, Austin AJ, Cammi R, Pomelli C, Ochterski JW, Ayala PY, Morokuma K, Voth GA, Salvador P, Dannenberg JJ, Zakrzewski VG, Dapprich S, Daniels AD, Strain MC, Farkas O, Malick DK, Rabuck AD, Raghavachari K, Foresman JB, Ortiz JV, Cui Q, Baboul AG, Clifford S, Cioslowski J, Stefanov BB, Liu G, Liashenko A, Piskorz P, Komaromi I, Martin RL, Fox DJ, Keith T, Al-Laham MA, Peng CY, Nanayakkara A, Challacombe M, Gill PMW, Johnson B, Chen W, Wong MW, Gonzalez C, Pople JA. *Gaussian 03, Revision B.03*. Gaussian Inc.: Pittsburgh PA, 2003.
18. Anderson JD, Paulsen ES, Dearden DV. *Int. J. Mass. Spectrom.* 2003; **227**: 63–76.
19. Saiful Islam M, Pethrick RA, Pugh D, Wilson MJ. *J. Chem. Soc., Faraday Trans.* 1997; **93**: 387–392.
20. Wilson MJ, Pethrick RA, Pugh D, Saiful Islam M. *J. Chem. Soc., Faraday Trans.* 1997; **93**: 2097–2104.
21. Wipff G, Weiner P, Kollman P. *J. Am. Chem. Soc.* 1982; **104**: 3249–3258.
22. Arnaud-Neu F, Delgado R, Chaves S. *Pure Appl. Chem.* 2003; **75**: 71–102.
23. Reed AE, Curtiss LA, Weinhold F. *Chem. Rev.* 1988; **88**: 899–926.
24. Hatchard CG, Parker CA. *Proc. Roy. Soc.* 1956; **A235**: 518–521.
25. Klotz IM, Ming W-CL. *J.Am.Chem.Soc.* 1953; **75**: 4159–4162.

DOI: 10.1002/poc